PROCEEDINGS OF SCIENCE

Search for Magnetic Monopoles with the Full ANTARES Neutrino Telescope Dataset

Ahmed Eddymaoui[a,*] **Jihad Boumaaza,**[a] **Juergen Brunner,**[b] **Abdelilah Moussa,**[c] **Bouchra Belhorma,**[d] **and Yahya Tayalati,**[a,d] **on behalf of the ANTARES Collaboration**

[a] *University Mohammed V in Rabat, Faculty of Sciences, 4 av. Ibn Battouta, B.P. 1014, R.P. 10000 Rabat, Morocco*

[b] *Aix Marseille Univ, CNRS/IN2P3, CPPM, Marseille, France*

[c] *University Mohammed I, Laboratory of Physics of Matter and Radiations, B.P.717, Oujda 6000, Morocco*

[d] *School of Applied and Engineering Physics, Mohammed VI Polytechnic University, Lot 660, Hay Moulay Rachid Ben Guerir, 43150, Morocco*

E-mail: sa96eddymaoui@gmail.com

This study presents a novel search for magnetic monopoles using data collected over a 14-year period (2008–2022) by the ANTARES neutrino telescope. The interaction of magnetic monopoles with matter was modeled using the Kasama, Yang, and Goldhaber cross-section. Upper limits on the flux of magnetic monopoles were derived for velocities both above and below the Cherenkov threshold. No events consistent with the passage of magnetic monopoles were detected, allowing to set an upper flux limit of 5.6×10^{-19} cm^{-2} s^{-1} sr^{-1} for ultra-relativistic monopoles and 3.4×10^{-18} cm^{-2} s^{-1} sr^{-1} for slow monopoles.

39th International Cosmic Ray Conference (ICRC2025)
15–24 July 2025
Geneva, Switzerland

ICRC 2025
The Astroparticle Physics Conference
Geneva July 15-24, 2025

[*] Speaker

1. Introduction

According to Grand Unified Theories (GUTs), magnetic monopoles are expected to have formed during a phase of symmetry breaking in the early universe. Over time, they would have been accelerated by galactic magnetic fields, acquiring significant momentum. These particles, having such high energies, might be able to pass through the Earth and produce observable signals in a Cherenkov-based detector, such as ANTARES (Astronomy with a Neutrino Telescope and Abyss environmental Research). Several searches for magnetic monopoles have already been carried out using neutrino telescopes. The ANTARES collaboration, for instance, published results based on data sets of 116 days [1], 1012 days [2], and 2480 days [3], while the IceCube collaboration also reported its findings in [4]. These results are shown in figure 4.
The present work builds upon these earlier efforts by analyzing a significantly larger dataset (3286 days) and employing an improved background rejection model. It represents the culmination of the ANTARES collaboration's search for magnetic monopoles, presenting the final results based on the full ANTARES data.

2. Magnetic Monopoles and Their Signals in Neutrino Telescopes

Magnetic monopoles are hypothetical particles carrying a single magnetic charge and are compelling predictions of theories that extend beyond the Standard Model, particularly Grand Unified Theories (GUTs). Dirac first demonstrated that the existence of even a single monopole would explain the quantization of electric charge [5]. Their magnetic charge g obeys the Dirac quantization condition, defined as an integer multiple of the fundamental unit g_D:

$$g = n\, g_D, \quad \text{with} \quad g_D = \frac{\hbar c}{2e} = \frac{e}{2\alpha} \approx 68.5\, e \tag{1}$$

Here, e denotes the elementary electric charge, c the speed of light in vacuum, $\hbar$ the Planck constant, and $\alpha \approx 1/137$ the fine-structure constant. Later, 't Hooft [6] and Polyakov [7] showed that monopoles naturally emerge as topologically stable solutions in any GUT where a simple gauge group breaks down to a subgroup containing U(1).
Magnetic monopoles traversing a medium emit light through several mechanisms: direct Cherenkov radiation, indirect Cherenkov emission from δ-rays, and luminescence. The dominant Cherenkov component is governed by the Frank–Tamm formula [8]:

$$\frac{d^2 N_\gamma}{dx\, d\lambda} = \frac{2\pi\alpha}{\lambda^2}\left(\frac{gn}{e}\right)^2\left(1 - \frac{1}{\beta^2 n^2}\right), \tag{2}$$

which applies when the monopole's speed exceeds the Cherenkov threshold ($\beta > c/n \approx 0.75$), resulting in a photon yield that increases with the monopole's velocity.
Monopoles therefore emit approximately 8200 times more Cherenkov photons than minimally ionizing electrically charged particles at the same velocity. Below the Cherenkov threshold, monopoles produce light primarily through δ-ray induced indirect emission, which is computed by integrating over the kinetic energy spectrum of secondary electrons, while Luminescence is modeled as being proportional to the monopole's energy loss, which becomes dominant in the velocity range $0.1 < \beta < 0.55$. The combined photon yield across these processes is plotted as a function of β in Figure 1.

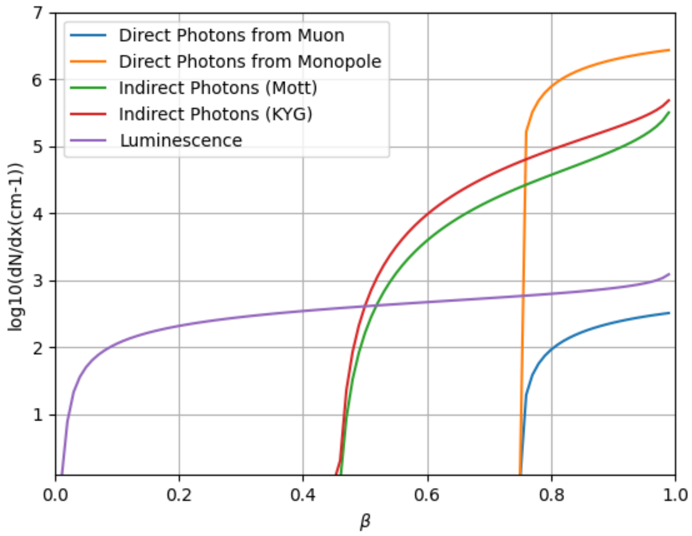

Figure 1: The figure shows the number of Cherenkov photons emitted per centimeter in seawater by a magnetic monopole carrying a Dirac charge (orange line), as well as by δ-rays generated along its trajectory, modeled using the Mott (green line) and KYG (red line) formalisms. Additionally, the contribution from luminescence processes is shown (magenta line). For comparison, the direct Cherenkov light yield from a relativistic muon is also displayed (blue line) as a reference.

3. Simulation

The magnetic monopole (MM) simulation was performed using the SIMON framework [9], developed by the ANTARES collaboration. It is based on the GENNEU and GEASIM Monte Carlo generators, which simulate monopole passage through the detector. In practice, GENNEUv5r1 and GEASIM v4r9 were used: GENNEU generates tracks on a cylindrical volume surrounding the detector for each velocity bin defined by the cut parameter, while GEASIM processes these tracks to produce the detector's response to monopoles with magnetic charge $g = g_D$. Photon emission, both direct and δ-ray induced Cherenkov light was simulated within the sensitive range of the ANTARES optical modules (300–800 nm). Monopoles were generated uniformly over the upper hemisphere and below the detector. The final simulated sample includes as up-going events with velocities in the interval $\beta \in [0.55, 0.995]$, subdivided into ten equal-width bins.

4. Event selection

To suppress the background from atmospheric muons and neutrinos, a set of selection criteria is applied. The first condition targets the zenith angle of reconstructed tracks, requiring $\theta_{\text{zenith}} \geq 90°$, which selects only up-going events, effectively using the Earth as a natural filter to eliminate downward-going background particles. The second condition ensures reconstruction quality by retaining only events with at least two detector lines ($n_{\text{lines}} \geq 2$). A further cut is applied on the track fit quality parameter, requiring $\chi^2 < 10$, in order to select well-reconstructed tracks. Additionally, the event selection favors track-like events by comparing the fit quality of track

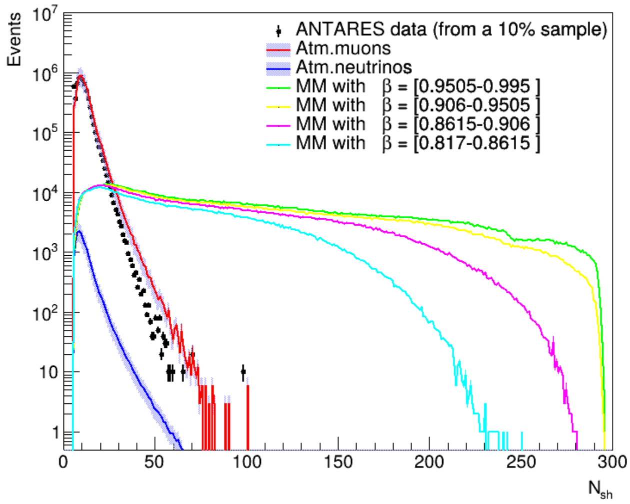

Figure 2: Distribution of N_{sh} for atmospheric muons (red histogram) and atmospheric neutrinos (blue histogram), with a 35% uncertainty band shown in gray. ANTARES data, based on a 10% burn sample, are also included for comparison. Simulated magnetic monopole signals are presented for four velocity intervals: $\beta \in [0.9505, 0.995]$ (green), $\beta \in [0.906, 0.9505]$ (yellow), $\beta \in [0.8615, 0.906]$ (magenta), and $\beta \in [0.817, 0.8615]$ (cyan).

hypotheses $t\chi^2$ to that of shower hypotheses $b\chi^2$, retaining events where the track fit is superior. The number of optical modules (storeys) with recorded hits, N_{sh}, is used as a discriminant variable, given that magnetic monopoles are expected to emit significantly more light than ionizing particles. To effectively combine reconstruction quality and brightness into a single variable, a parameter α is defined as:

$$\alpha = \frac{t\chi^2}{1.3 + \left(0.04 \times \left(N_{sh} - N_{df}\right)\right)^2}, \tag{3}$$

where N_{df} is the number of degrees of freedom in the fit, the α parameter enhances the separation of magnetic monopole signals from background by penalizing poorly reconstructed or low-brightness events. A comparison of the N_{sh} and α distributions between data and simulation shows good agreement, validating the selection strategy.

5. Event Selection Optimization and Background Modeling

To estimate the residual background, the low-statistics tail of the N_{sh} distribution of atmospheric muons is modeled by fitting a Landau function and extrapolating into the signal region. This fit, combined with the atmospheric muon rate defined in equation 4, yields the total expected background used in the sensitivity evaluation.

$$N_{\mathrm{atm,muon}}(N_{\mathrm{sh,cut}}, \alpha_{\mathrm{cut}}) = \int_{N_{\mathrm{sh,cut}}}^{\infty} \mathrm{Landau}(N_{\mathrm{sh}})\, dN_{\mathrm{sh}} \cdot \frac{\int_0^{\alpha_{\mathrm{cut}}} N_{\mathrm{ev}}(\alpha)\, d\alpha}{\int_0^{\infty} N_{\mathrm{ev}}(\alpha)\, d\alpha} \tag{4}$$

The analysis optimizes the sensitivity to magnetic monopoles by tuning selection cuts separately for each velocity bin. The 90% confidence level sensitivity is calculated according to the Feldman–Cousins approach applied to a Poisson-distributed events.

$$S_{90\%}\,[\mathrm{cm}^{-2}\ \mathrm{s}^{-1}\ \mathrm{sr}^{-1}] = \frac{\bar{\mu}_{90}\,(n_b)}{A_{eff}\left[\mathrm{cm}^2\ \mathrm{sr}\right] \times T\,[\mathrm{s}]}, \tag{5}$$

where T is the duration of data taking, n_b representing the number of expected background events in the 90% C.L. interval (μ_{90}), $\bar{\mu}_{90}$ and A_{eff} are defined as:

$$\bar{\mu}_{90}\,(n_b) = \sum_{n_{obs}=0}^{\infty} \mu_{90} \frac{n_b^{n_{obs}}}{n_{obs}!} e^{-n_b}, \tag{6}$$

$$A_{eff} = \frac{n_{MM}}{\Phi_{MM}}, \tag{7}$$

with N_{MM} is the number of simulated magnetic monopoles surviving all selection criteria, and Φ_{MM} is the generated flux. The selection cuts are systematically adjusted to find the configuration that yields the lowest flux upper limit in each velocity range.

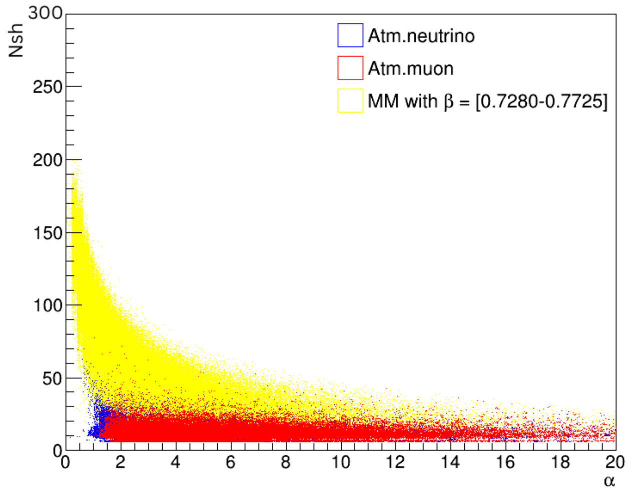

Figure 3: Scatter plot of the two discriminant variables, α and N_{sh}. Magnetic monopole signals simulated for a velocity range of $\beta \in [0.7280,\ 0.7725]$ are shown in yellow, while background events from atmospheric muons and neutrinos are displayed in red and blue, respectively.

6. Results

The optimized selection criteria for each velocity interval are summarized in Table 1. In the high-velocity regime ($\beta_{\mathrm{reco}} = 1$), the expected background lies between 1.24 and 1.67 events, with zero events observed. In the low-velocity region, there β_{reco} is a fitted parameter, the predicted background ranges from 0.76 to 1.70 events. Only a single event was observed, and this was within the interval $[0.6490,\ 0.6835] \pm 5\%$. For all other intervals, the observed counts do not exceed the expected background, consistent with the conservative approach adopted in this analysis. Flux upper limits at 90% confidence level (C.L.) were computed per interval as detailed in the previous section. As no signal excess was found, the resulting limits match the expected sensitivities under the background hypothesis. Results are compiled in Table 1, based on the full 14-year ANTARES dataset with a livetime of 3286 days.

β Interval	β_{reco}	β cut	α cut	N_{sh} cut	Flux upper limit $[cm^{-2}\ s^{-1}\ sr^{-1}]$
[0.9505, 0.9950]	1	-	< 0.3	≥ 105	5.6×10^{-19}
[0.9060, 0.9505[	1	-	< 0.3	≥ 105	6.7×10^{-19}
[0.8615, 0.9060[	1	-	< 0.3	≥ 105	1.1×10^{-18}
[0.8170, 0.8615[	1	-	< 0.6	≥ 102	2.6×10^{-18}
[0.7725, 0.8170[	Fitted	[0.7725, 0.8170[±5%	< 1	≥ 124	3.4×10^{-18}
[0.7280, 0.7725[	Fitted	[0.7280, 0.7725[±5%	< 2.6	≥ 94	3.1×10^{-18}
[0.6835, 0.7280[	Fitted	[0.6835, 0.7280[±5%	< 4	≥ 78	3.2×10^{-18}
[0.6390, 0.6835[	Fitted	[0.6390, 0.6835[±5%	< 6.6	≥ 66	3.0×10^{-18}
[0.5945, 0.6390[	Fitted	[0.5945, 0.6390[±5%	< 8.2	≥ 54	5.8×10^{-18}
[0.5500, 0.5945[	Fitted	[0.5500, 0.5945[±5%	< 9	≥ 50	8.0×10^{-18}

Table 1: Summary of optimized selection cuts, expected background, observed events, and 90% C.L. flux upper limits for each β interval, using 3286 live days of ANTARES data.

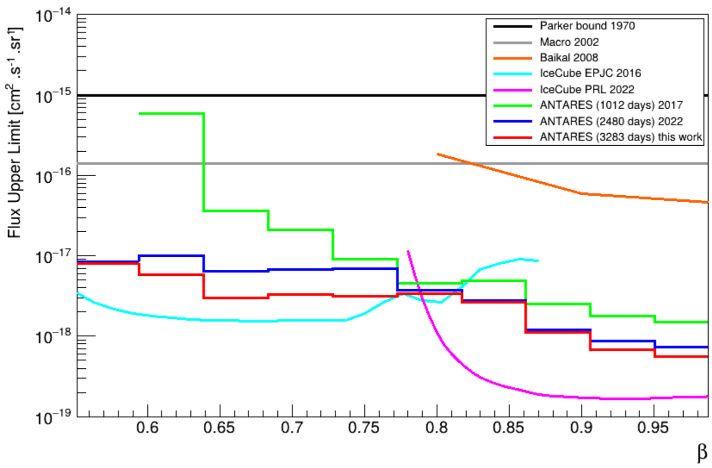

Figure 4: The 90% confidence level upper limits on the flux of magnetic monopoles obtained with the ANTARES neutrino telescope, based on 14 years of data corresponding to 3286 live days (red line). For context, these results are compared with those from previous ANTARES analyses (green [2] and blue lines [3]), as well as with constraints reported by other experiments, including IceCube (cyan [4] and magenta [10]), MACRO (gray [11]), and Baikal (orange [12]). The theoretical Parker bound is also shown for reference (black line [13]).

7. Conclusion

In this work, we have presented the final results of the search for magnetic monopoles using the complete ANTARES dataset, corresponding to 3286 days of livetime recorded between 2008 and 2022. The analysis covered magnetic monopoles with velocities in the range $\beta \in [0.57, 0.995]$, and employed the BBFit algorithm [14] for event reconstruction, in combination with the latest Run-By-Run Monte Carlo simulations provided by the ANTARES collaboration. No candidate events survived the selection cuts across any of the ten defined velocity intervals. Consequently, 90% C.L. upper limits on the monopole flux were derived for each interval. Notably, the sensitivity at low velocities shows a marked improvement compared to previous ANTARES results. This enhancement is primarily attributed to the application of a relaxed velocity cut in that region, as well as the conservative approach adopted for background estimation and rejection.

Aknowledgements

The authors acknowledge the financial support of the funding agencies: Centre National de la Recherche Scientifique (CNRS), Commissariat à l'énergie atomique et aux énergies alternatives (CEA), Commission Européenne (FEDER fund and Marie Curie Program), LabEx UnivEarthS (ANR-10-LABX-0023 and ANR-18-IDEX-0001), Région Alsace (contrat CPER), Région Provence-Alpes-Côte d'Azur, Département du Var and Ville de La Seyne-sur-Mer, France; Bundesministerium für Bildung und Forschung (BMBF), Germany; Istituto Nazionale di Fisica Nucleare (INFN), Italy; Nederlandse organisatie voor Wetenschappelijk Onderzoek (NWO), the Netherlands; Ministry of Education and Scientific Research, Romania; MCIN for PID2021-124591NB-C41, -C42, -C43 and PDC2023-145913-I00 funded by MCIN/AEI/10.13039/501100011033 and by "ERDF A way of making Europe", for ASFAE/2022/014 and ASFAE/2022 /023 with funding from the EU NextGenerationEU (PRTR-C17.I01) and Generalitat Valenciana, for Grant AST22_6.2 with funding from Consejería de Universidad, Investigación e Innovación and Gobierno de España and European Union - NextGenerationEU, for CSIC-INFRA23013 and for CNS2023-144099, Generalitat Valenciana for CIDEGENT/2020/049, CIDEGENT/2021/23, CIDEIG/2023/20, ESGENT2024/24, CIPROM/2023/51, GRISOLIAP/2021/192 and INNVA1/2024/110 (IVACE+i), Spain; Ministry of Higher Education, Scientific Research and Innovation, Morocco, and the Arab Fund for Economic and Social Development, Kuwait. We also acknowledge the technical support of Ifremer, AIM and Foselev Marine for the sea operation and the CC-IN2P3 for the computing facilities.

References

[1] S. Adrián-Martínez et al., Search for relativistic magnetic monopoles with the ANTARES neutrino telescope, Astroparticle Physics 35 (10) (2012) 634–640. arXiv:1110.2656, doi:10.1016/j.astropartphys.2012.02.007.

[2] A. Albert et al., Search for relativistic magnetic monopoles with five years of the ANTARES detector data, Journal of High Energy Physics 07 (07) (2017) 054. arXiv:1703.00424, doi:10.1007/jhep07(2017)054.

[3] A. Albert et al., Search for magnetic monopoles with ten years of the ANTARES neutrino telescope, Journal of High Energy Astrophysics 34 (10) (2022) 1–8. arXiv:2202.13786, doi:10.1016/j.jheap.2022.03.001.

[4] M.G. Aartsen et al., Searches for relativistic magnetic monopoles in IceCube, The European Physical Journal C 76 (3) (2016) 133. arXiv:1511.01350, doi:10.1140/epjc/s10052-016-3953-8.

[5] P. A. M. Dirac, Quantised singularities in the electromagnetic field, Proc. Roy. Soc. Lond. A 133 (821) (1931) 60–72. doi:10.1098/rspa.1931.0130.

[6] G. 't Hooft, Magnetic Monopoles in Unified Gauge Theories, Nucl. Phys. B 79 (1974) 276–284. doi:10.1016/0550-3213(74)90486-6.

[7] A. M. Polyakov, Particle Spectrum in Quantum Field Theory, JETP Lett. 20 (1974) 194–195.

[8] D. R. Tompkins, Total energy loss and Čerenkov emission from monopoles, Phys. Rev. 138 (1965) B248–B250. doi:10.1103/PhysRev.138.B248.

[9] B. A. P. van Rens, Magnetic monopoles simulation, Internal Note ANTARES-SOFT-2006-005, ANTARES Collaboration (2006).

[10] R. Abbasi et al., Search for relativistic magnetic monopoles with eight years of IceCube data, Physical Review Letters 128 (5) (2022) 051101. arXiv:2109.13719, doi:10.1103/physrevlett.128.051101.

[11] M. Ambrosio et al., Final results of magnetic monopole searches with the MACRO experiment, The European Physical Journal C 25 (4) (2002) 511–522. arXiv:hep-ex/0207020, doi:10.1140/epjc/s2002-01046-9.

[12] V. Aynutdinov et al., Search for relativistic magnetic monopoles with the Baikal neutrino telescope, Astroparticle Physics 29 (6) (2008) 366–372. doi:10.1016/j.astropartphys.2008.03.006.

[13] E. N. Parker, The Origin of Magnetic Fields, Astrophys. J. 160 (1970) 383. doi:10.1086/150442.

[14] J. A. Aguilar et al., A fast algorithm for muon track reconstruction and its application to the ANTARES neutrino telescope, Astroparticle Physics 34 (9) (2011) 652–662. arXiv:1105.4116, doi:10.1016/j.astropartphys.2011.01.003.

Full Authors List: The ANTARES Collaboration

A. Albert[a,b], S. Alves[c], M. André[d], M. Ardid[e], S. Ardid[e], J.-J. Aubert[f], J. Aublin[g], B. Baret[g], S. Basa[h], Y. Becherini[g], B. Belhorma[i], F. Benfenati[j,k], V. Bertin[f], S. Biagi[l], J. Boumaaza[m], M. Bouta[n], M.C. Bouwhuis[o], H. Brânzaş[p], R. Bruijn[o,q], J. Brunner[f], J. Busto[f], B. Caiffi[r], D. Calvo[c], S. Campion[s,t], A. Capone[s,t], F. Carenini[j,k], J. Carr[f], V. Carretero[c], T. Cartraud[g], S. Celli[s,t], L. Cerisy[f], M. Chabab[u], R. Cherkaoui El Moursli[m], T. Chiarusi[j], M. Circella[v], J.A.B. Coelho[g], A. Coleiro[g], R. Coniglione[l], P. Coyle[f], A. Creusot[g], A.F. Díaz[w], B. De Martino[f], C. Distefano[l], I. Di Palma[s,t], C. Donzaud[g,x], D. Dornic[f], D. Drouhin[a,b],

T. Eberl[y], A. Eddymaoui[m], T. van Eeden[o], D. van Eijk[o], S. El Hedri[g], N. El Khayati[m], A. Enzenhöfer[f], P. Fermani[s,t], G. Ferrara[l], F. Filippini[j,k], L. Fusco[z], S. Gagliardini[s,t], J. García-Méndez[e], C. Gatius Oliver[o], P. Gay[y,g], N. Geißelbrecht[y], H. Glotin[aa], R. Gozzini[c], R. Gracia Ruiz[y], K. Graf[y], C. Guidi[r,ab], L. Haegel[g], H. van Haren[ac], A.J. Heijboer[o], Y. Hello[ad], L. Hennig[y], J.J. Hernández-Rey[c], J. Hößl[y], F. Huang[f], G. Illuminati[j,k], B. Jisse-Jung[o], M. de Jong[o,ae], P. de Jong[o,q], M. Kadler[af], O. Kalekin[y], U. Katz[y], A. Kouchner[g], I. Kreykenbohm[ag], V. Kulikovskiy[r], R. Lahmann[y], M. Lamoureux[g], A. Lazo[c], D. Lefèvre[ah], E. Leonora[ai], G. Levi[j,k], S. Le Stum[f], S. Loucatos[aj,g], J. Manczak[c], M. Marcelin[h], M. Marconi[r,ab], A. Margiotta[j,k], A. Marinelli[ak,al], J.A. Martínez-Mora[e], P. Migliozzi[ak], A. Moussa[n], R. Muller[o], S. Navas[am], E. Nezri[h], B. Ó Fearraigh[o], E. Oukacha[g], A.M. Păun[p], G.E. Păvălaş[p], S. Peña-Martínez[g], M. Perrin-Terrin[f], P. Piattelli[l], C. Poirè[z], V. Popa[p], T. Pradier[a], N. Randazzo[ai], D. Real[c], G. Riccobene[l], A. Romanov[r,ab], A. Sánchez Losa[c], A. Saina[c], F. Salesa Greus[c], D.F.E. Samtleben[o,ae], M. Sanguineti[r,ab], P. Sapienza[l], F. Schüssler[aj], J. Seneca[o], M. Spurio[j,k], Th. Stolarczyk[aj], M. Taiuti[r,ab], Y. Tayalati[m,an], B. Vallage[aj,g], G. Vannoye[f], V. Van Elewyck[g,ao], S. Viola[l], D. Vivolo[ap,ak], J. Wilms[ag], S. Zavatarelli[r], A. Zegarelli[s,t], J.D. Zornoza[c], J. Zúñiga[c].

[a] Université de Haute Alsace, F-68100 Mulhouse, France
[b] Université de Strasbourg, CNRS, IPHC UMR 7178, France
[c] IFIC - Instituto de Física Corpuscular (CSIC - Universitat de València), c/ Catedrático José Beltrán, 2 E-46980 Paterna, Valencia, Spain
[d] Technical University of Catalonia, Laboratory of Applied Bioacoustics, Rambla Exposició, 08800 Vilanova i la Geltrú, Barcelona, Spain
[e] Institut d'Investigació per a la Gestió Integrada de les Zones Costaneres (IGIC) - Universitat Politècnica de València. C/ Paranimf 1, 46730 Gandia, Spain
[f] Aix Marseille Univ, CNRS/IN2P3, CPPM, Marseille, France [g] Université Paris Cité, CNRS, Astroparticule et Cosmologie, F-75013 Paris, France
[h] Aix Marseille Univ, CNRS, CNES, LAM, Marseille, France [i] National Center for Energy Sciences and Nuclear Techniques, B.P.1382, R. P.10001 Rabat, Morocco
[j] INFN - Sezione di Bologna, Viale Berti-Pichat 6/2, 40127 Bologna, Italy
[k] Dipartimento di Fisica e Astronomia dell'Università di Bologna, Viale Berti-Pichat 6/2, 40127, Bologna, Italy
[l] INFN - Laboratori Nazionali del Sud (LNS), Via S. Sofia 62, 95123 Catania, Italy
[m] University Mohammed V in Rabat, Faculty of Sciences, 4 av. Ibn Battouta, B.P. 1014, R.P. 10000 Rabat, Morocco
[n] University Mohammed I, Laboratory of Physics of Matter and Radiations, B.P.717, Oujda 6000, Morocco
[o] Nikhef, Science Park, Amsterdam, The Netherlands
[p] Institute of Space Science - INFLPR subsidiary, 409 Atomistilor Street, Măgurele, Ilfov, 077125 Romania
[q] Universiteit van Amsterdam, Instituut voor Hoge-Energie Fysica, Science Park 105, 1098 XG Amsterdam, The Netherlands
[r] INFN - Sezione di Genova, Via Dodecaneso 33, 16146 Genova, Italy
[s] INFN - Sezione di Roma, P.le Aldo Moro 2, 00185 Roma, Italy
[t] Dipartimento di Fisica dell'Università La Sapienza, P.le Aldo Moro 2, 00185 Roma, Italy
[u] LPHEA, Faculty of Science - Semlali, Cadi Ayyad University, P.O.B. 2390, Marrakech, Morocco
[v] INFN - Sezione di Bari, Via E. Orabona 4, 70126 Bari, Italy
[w] Department of Computer Architecture and Technology/CITIC, University of Granada, 18071 Granada, Spain
[x] Université Paris-Sud, 91405 Orsay Cedex, France
[y] Friedrich-Alexander-Universität Erlangen-Nürnberg, Erlangen Centre for Astroparticle Physics, Erwin-Rommel-Str. 1, 91058 Erlangen, Germany
[z] Università di Salerno e INFN Gruppo Collegato di Salerno, Dipartimento di Fisica, Via Giovanni Paolo II 132, Fisciano, 84084 Italy
[aa] LIS, UMR Université de Toulon, Aix Marseille Université, CNRS, 83041 Toulon, France
[ab] Dipartimento di Fisica dell'Università, Via Dodecaneso 33, 16146 Genova, Italy
[ac] Royal Netherlands Institute for Sea Research (NIOZ), Landsdiep 4, 1797 SZ 't Horntje (Texel), the Netherlands
[ad] Géoazur, UCA, CNRS, IRD, Observatoire de la Côte d'Azur, Sophia Antipolis, France
[ae] Huygens-Kamerlingh Onnes Laboratorium, Universiteit Leiden, The Netherlands
[af] Institut für Theoretische Physik und Astrophysik, Universität Würzburg, Emil-Fischer Str. 31, 97074 Würzburg, Germany
[ag] Dr. Remeis-Sternwarte and ECAP, Friedrich-Alexander-Universität Erlangen-Nürnberg, Sternwartstr. 7, 96049 Bamberg, Germany
[ah] Mediterranean Institute of Oceanography (MIO), Aix-Marseille University, 13288, Marseille, Cedex 9, France; Université du Sud Toulon-Var, CNRS-INSU/IRD UM 110, 83957, La Garde Cedex, France
[ai] INFN - Sezione di Catania, Via S. Sofia 64, 95123 Catania, Italy
[aj] IRFU, CEA, Université Paris-Saclay, F-91191 Gif-sur-Yvette, France
[ak] INFN - Sezione di Napoli, Via Cintia 80126 Napoli, Italy
[al] Dipartimento di Fisica dell'Università Federico II di Napoli, Via Cintia 80126, Napoli, Italy
[am] Dpto. de Física Teórica y del Cosmos & C.A.F.P.E., University of Granada, 18071 Granada, Spain
[an] School of Applied and Engineering Physics, Mohammed VI Polytechnic University, Lot 660, Hay Moulay Rachid Ben Guerir, 43150, Morocco
[ao] Institut Universitaire de France, 75005 Paris, France
[ap] Dipartimento di Matematica e Fisica dell'Università della Campania L. Vanvitelli, Via A. Lincoln, 81100, Caserta, Italy